JOURNAL OF MATERIALS SCIENCE: MATERIALS IN MEDICINE **10** (1999) 481–484

Characterization of SiO_2–Na_2O–Fe_2O_3–CaO–P_2O_5–B_2O_3 glass ceramics

K. SINGH*, D. BAHADUR
Department of Metallurgical Engineering and Materials Science, I.I.T. Powai, Bombay-400076, India

Bioactivity and magnetic properties were investigated in glass and glass ceramics based on the SiO_2–Na_2O–Fe_2O_3–CaO–P_2O_5–B_2O_3 system to find their suitability as thermoseed for hyperthermia treatment of cancer. The effect of change in compositions on bioactivity was examined in simulated body fluids. The glass ceramic samples exhibit $Na_3CaSi_3O_8$ and $Na_{3-X}Fe_XPO_4$ phases. After dipping the glass ceramic samples in simulated body fluids silica hydrogel first forms, followed by an amorphous calcium phosphate layer. Magnetic and microwave resonance experiments further demonstrate the potential of these glass ceramics for possible use in hyperthermia.

1. Introduction

There has been increasing interest in bioactive glass and glass ceramics in the past two decades due to their critical structural applications within the human body. Recently, these bioactive glass and glass ceramic materials have been receiving attention as bone bonding materials [1–4]. The bonding of bioactive glass and glass ceramics to bone tissue was associated with a series of chemical interactions at the interface with the surrounding fluids and tissue. Hench [5] has described the bonding mechanism as a sequence of reactions between the glass and the surrounding fluid. A silicon-rich layer was formed initially, followed by the formation of a calcium-phosphate-rich layer [4]. Based on these properties of glass ceramics, it can be expected that glass ceramics containing a magnetic phase with a glassy matrix, could be used as thermosed for hyperthermia treatment of cancer [6]. Hyperthermia treatment of cancer uses bioactive glass ceramics containing a magnetic phase, which is exposed to an alternating magnetic field, by which heat is generated due to hystersis loss. Hyperthermia treatment may also be performed by other means, e.g. microwave power, etc. Generally, the tumor is heated more than the surrounding normal tissues, since blood vessels and the nervous system are poorly developed in the tumor and blood flow is not normal. So, hyperthermia treatment is considered to be an effective treatment for cancer without side effects and this process can be repeated many times after implanting a bioactive and biocompatible glass ceramic into the body. Luderer *et al.* [7] have shown that a glass ceramic with lithium ferrite ($LiFe_5O_8$) and magnetite (Fe_3O_4) in an Al_2O_3–SiO_2–P_2O_5 glassy matrix could be used as a thermoseed for hyperthermia treatment of cancer. Here we report the synthesis and characterization of structural bioactive and magnetic properties of different compositions of glass and glass ceramics in SiO_2–Na_2O–CaO–P_2O_5–B_2O_3–Fe_2O_3 systems.

2. Materials and methods

The glasses were synthesized by mixing, calcining and melting a stoichiometric amount of reagent grade chemicals of $Fe_2O_3, CaCO_3, Na_2CO_3, CaH \cdot PO_4 \cdot H_2O$, SiO_2 and H_3BO_4. The details of the compositions, and their labels before and after ceramizing are given in Table I. X-ray diffraction (XRD) measurements were performed by a Phillips PW1820 diffractrometer using CuK_α radiation with Ni filter. Differential thermal analysis (DTA) measurement was done to find out the glass transition and crystallization temperatures from the glass. Measurement of electron paramagnetic resonance (EPR) was carried out in the X-band frequency region using a Varian associates EPR spectrometer at room temperature. The bioactivity of glass ceramic samples was checked in simulated body fluids (SBF) solution, in which the ion concentrations were made nearly equal to those in human blood plasma [8]. The preparation details of SBF solution are given elsewhere [6]. The glass ceramic samples were immersed in the SBF solution for different time periods. The fluid was taken out to analyze the concentration of elements by inductively coupled plasma (ICP) emission spectroscopy. The dipped sample surfaces (in SBF solution) were polished and coated with carbon for scanning electron microscopy (SEM, Camscan) as well as elemental analysis by EDAX

---

*Present address: Institute für Werkstoffe der Energietechnik, IWE 1, Forschungszentrum Jülich, D-52425 Jülich, Germany

0957–4530 © *1999 Kluwer Academic Publishers*

TABLE I Nominal compositions of glasses

	Composition (wt %)						Label of glass	Label of glass ceramic
	SiO_2	Na_2O	Fe_2O_3	CaO	P_2O_5	B_2O_3		
1	45	22	15	8	7	3	15 Fe	15 FeH
2	48.2	25	10.3	6.5	7	3	10 Fe	10 FeH
3	50	27	5	8	7	3	5 Fe	5 FeH

measurements. Magnetic measurements were carried out by a vibrating sample magnetometer (VSM) to obtain information regarding the magnetic phase in the glass ceramic samples.

3. Results and discussion

The XRD patterns of the as-quenched samples exhibit only broad hallow indicating the amorphous nature in all samples. The DTA plot of the glass samples gives an estimate of the glass transition, T_g, and growth, T_c, temperatures. The T_gs of samples with 15 Fe, 10 Fe and 5 Fe (in weight per cent) are observed at 520, 545 and 595 °C, whereas T_c occurs at 610, 700 and 745 °C, respectively. Based on DTA results, all three glass samples were heated around 50 °C above T_g for nucleation and held for 1 h and then heated further to their T_c for crystallization and held for 24 h.

Typical XRD patterns of glass (5 Fe), glass ceramic (5 FeH) and dipped glass ceramic (5 FeHD, dipped for 36 days in SBF solution) samples are shown in Fig. 1. The glass ceramic samples exhibit $Na_2CaSi_3O_8$ as the main phase. Besides, there are lines that can be identified as due to $Na_{3-X}Fe_XPO_4$ (solid solution based on Na_3PO_4) [9]. However, the XRD peaks are broad. This broadness is more prominent in 15 FeH compared with that of 10 FeH and 5 FeH samples. It indicates that the extent of crystallization is less in 15 FeH compared with 10 FeH and 5 FeH. After dipping glass ceramic samples in SBF solution, no change is observed in the XRD pattern of the soaked glass ceramic sample 10 FeH. In contrast, the XRD patterns of samples 5 FeH and 15 FeH exhibit completely amorphous nature after dipping in SBF solution.

The glass ceramic samples were polished and dipped in 50 ml SBF solution for 36-day time periods. Fig. 2a and b show surface compositional profiles for samples 10 FeHD and 5 FeHD, respectively. The change in elemental concentration of the SBF solution after soaking glass ceramic samples for 36 days and the weight loss of the samples are given in Table II.

The weight loss of samples in SBF solution increases with decreasing iron contents in the sample. Silicate ions dissolve from all the samples. The silicate ion dissolution trend in SBF solution is more pronounced in 5 FeH

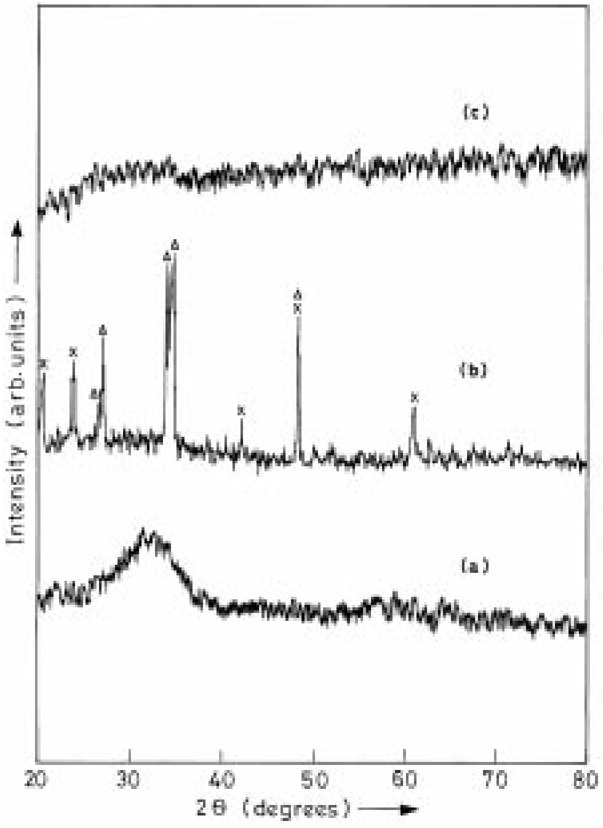

Figure 1 XRD patterns of (a) 5 Fe, (b) 5 FeH and (c) 5 FeHD (after dipping in SBF solution for 36 days): (Δ) $Na_2CaSi_3O_8$, (X) $Na_{3-X}Fe_XPO_4$.

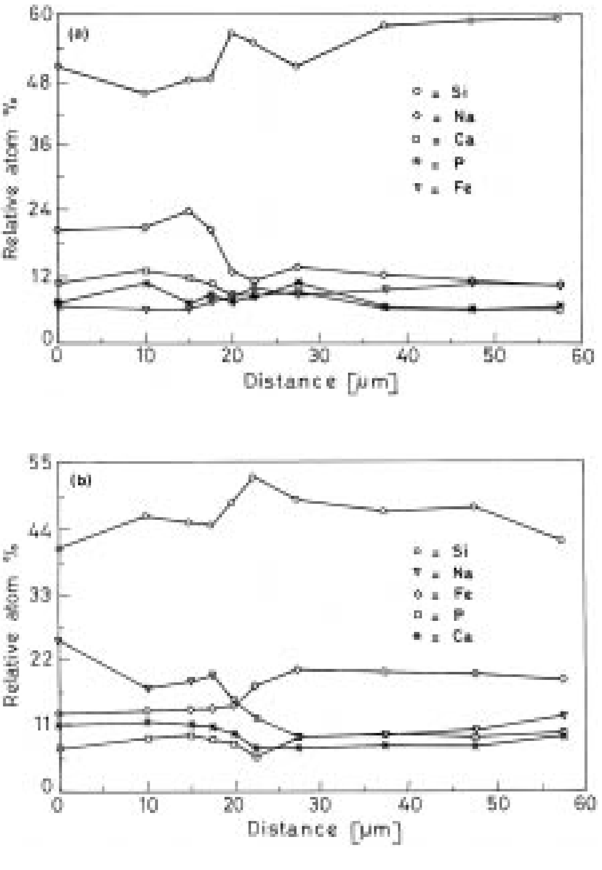

Figure 2 Compositional profiles of the surface layer of samples 10 FeHD(a) and 5 FeHD(b).

TABLE II Change in concentration of SBF solution and weight loss of glass ceramic samples after 36-days soaking in SBF

Label	Ion concentration (p.p.m.)				Weight loss ($mg\,g^{-1}$)
	Si	P	Ca	Na	
SBF (pure)	0.8	25.4	80.7	3451	—
15 FeH	5.6	33.5	83.5	3362	13
10 FeH	5.6	22	80	3685	16
5 FeH	12	38	84	3298	40

compared with the other two samples, as shown in Table II. Dissolution of phosphate ions was observed from samples 15 FeH and 5 FeH; whereas for sample 10 FeH, the SBF fluid concentration decreased by 3 p.p.m. compared with the pure SBF fluid. The dissolution of phosphate ions from glass and glass ceramics has also been reported by Kim *et al.* [10] and Kokubo [11] in P_2O_5-containing glasses. The percentage of calcium ions increases in SBF after 36 days of soaking for 15 FeH and 5 FeH samples. The dissolution of Si and P ions in SBF solution shows the same trend in 15 FeH and 5 FeH glass ceramic samples. Interestingly, the XRD patterns of both the soaked samples are also identical. This indicates that the dissolved silicate and calcium along with phosphate ions play an important role in forming silica hydrogel first and then a calcium phosphate amorphous layer on the surfaces of samples 15 FeH and 5 FeH. But, no crystalline apatite layer was formed on their surfaces after soaking, as observed from the XRD pattern of both samples. It is reported that silicon plays an essential role in the initial stage of apatite formation [12]. Calcium ions dissolved from the glass ceramics increase the ionic activity of apatite in the surrounding body fluid. The hydrated silica formed on the ion surfaces provide favorable sites for apatite nucleation. Once the apatite nuclei are formed, they grow spontaneously by consuming calcium and phosphate ions from the surrounding fluid, since the body fluid is already supersaturated with respect to apatite even under normal conditions [13]. For sample 10 FeH, the calcium concentration was unchanged and took few phosphate ions from the fluids. EDX analysis of this sample also shows no change in the atomic percentage of calcium and phosphate ions. This indicates that the dissolution of calcium ions plays an important role in forming the apatite layer on the surfaces of glass and glass ceramics [14]. Dissolution of silicate and phosphate ions from the samples is suppressed by the Fe_2O_3 concentration. It is already known that Fe_2O_3 effectively increases the chemical durability of glasses [15]. Basically, the solubility of glass and glass ceramics is suppressed by Fe_2O_3 and SiO_2. On the other hand Na_2O and P_2O_5 will be responsible for enhancing the solubility [15]. When the concentration of Na_2O and P_2O_5 increases in the sample, the Na^+ and P^{+5} ions will dissolve, increasing pH and the degree of supersaturation of the surrounding fluid with respect to apatite, and thus enhancing the rate of apatite formation. In fact, the increment in SiO_2 concentration in samples is known to increase glass durability. But in the present case, the iron concentration seems to play a vital role in increasing the durability of the samples. Weight loss increases with decreasing percentage of Fe_2O_3 in nominal compositions after immersion in SBF solution. Less weight loss was observed in high Fe_2O_3-containing samples. These results show that the glass ceramic became more bioactive following addition of Na_2O and P_2O_5, but less bioactive following addition of B_2O_3 and Fe_2O_3.

Microwave resonance studies on glasses and glass ceramics containing varying amounts of iron have been done to demonstrate the absorption of microwave power by the sample and to obtain information regarding valence state and symmetry of iron ions. Spectra for glass and glass ceramics samples are shown in Fig. 3a and b, respectively. The spectra of glass samples exhibit resonances at $g = 2.0$ and 4.2. In crystalline samples, the $g = 4.2$ line is not seen and the line width, $\Delta H_{1/2}$, of the absorption line at $g = 2.1$ is considerably narrow in 15 FeH and 10 FeH. However, both the resonances are present in the 5 FeH sample. The disappearance of the $g = 4.1$ line in the crystalline samples would mean a decrease of low symmetry Fe^{+3} sites, since $g = 4.2$ resonance in the EPR spectra is due to Fe^{+3} ions in low symmetry sites [17]. Narrowing of the $g = 2.1$ line occurs after heat treatment (15 FeH and 5 FeH samples). Consequently, the difference between the line width in the glass and glass ceramics seems to represent mostly the change in symmetry/co-ordination of Fe^{+3} ions from the glassy to crystalline state [18].

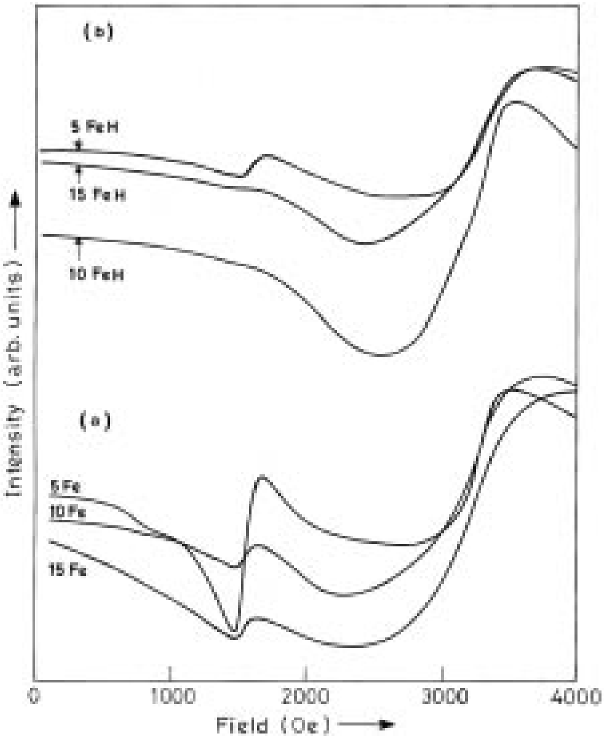

Figure 3 EPR spectra of (a) glass and (b) glass ceramic samples.

TABLE III Magnetic parameters of glass ceramic samples

Sample	H_c(Oe)	M_s^a(emu g^{-1})
15 FeH	625	0.42
10 FeH	500	0.31
5 FeH	650	0.21

[a] At 12 kOe (not saturated).

The magnetic properties of glass ceramic samples 15 FeH, 10 FeH and 5 FeH are summarized in Table III. Magnetization is not saturated up to a field of 12 kOe. As expected magnetic moments decrease with decreasing iron concentration in samples. The value of magnetic moments is very small with high coercive forces in all the samples. In the present samples the magnetic phase is possibly $Na_{31-X}Fe_XPO_4$ as confirmed by XRD measurement. Since, the concentration of iron oxide in these glasses is very small and it is very difficult to ascertain the value of the iron substitution in $Na_{3-X}Fe_XPO_4$, the magnetic moments cannot be estimated. High coercive forces have been reported in precipitated glasses due to larger stresses and smaller magnetic interaction among the magnetic particles of the crystallized glasses [19]. In general, ferrimagnetic materials generate heat in an amount proportional to the area of the magnetic hystersis loop and the frequency of the alternating applied magnetic field. The area of the hysteresis loop is very small in the present samples due to the small magnetic moments, as shown in Table III. The amount of heat generation decreases with iron content. 15 FeH shows the maximum hystersis area compared with 10 FeH and 5 FeH samples.

4. Conclusions

The effect of change in glass composition on the crystallization, bioactivity and magnetic properties is investigated. For samples 15 FeH and 5 FeH, an initially Si-rich layer forms followed by the formation of an amorphous calcium-phosphate-rich layer on their surfaces after soaking in SBF solution. However, an amorphous layer is not formed on the surface of sample 10 FeH. High coercive force and small magnetic moments were observed in all the samples. Magnetic moment decreases with increased iron concentration.

Acknowldgments

This work was financially supported by Council of Scientific and Industrial Research, Government of India.

References

1. L. L. HENCH, R. J. SPLINTER, W. C. ALLANI and T. K. GREENLEE, *J. Biomed. Res. Symp.* **2** (1971) 117.
2. T. KITSUGI, T. YAMAMURA, T. NAKAMURA and T. KOKUBO, *J. Biomed. Mater. Res.* **23** (1989) 631.
3. K. OHARA, T. NAKAMURA, T. YAMAMURA, T. KOKUBO, Y. EBISAWA, Y. KOTORA and K. OKA, *ibid.* **25** (1991) 357.
4. T. KOKUBO, S. ITO, Z. T. HUANG, T. HAYASHI, M. SHIGEMATA, S. SASKKA, T. KITSUGI and T. YAMAMURA, *ibid.* **24** (1990) 331.
5. L. L. HENCH, *J. Amer. Ceram. Soc.* **74** (1991) 1487.
6. Y. EBISAWA, T. KOKUBO, K. OHURA and T. YAMAMURA, *J. Mater. Sci. Mater. Med.* **1** (1990) 239.
7. A. A. LUDERER, N. F. BORRELLI, J. N. PANZARINA, G. R. MANSFIELD, D. M. HESS, J. L. BROWN and E. H. BARNELL, *Radiation Res.* **4** (1983) 190.
8. J. GAMBLE, in ‘‘Chemical Anatomy, Physiology and Pathology of Extracellular Fluid’’, (Harvard University Press, Cambridge, MA, 1967) p. 1.
9. B. I. LAZORYAK, S. YU ORALKOV and R. G. AZIEV, *Russian J. Inorg. Chem.* **33** (1988), 252.
10. H. KIM, F. MAYAJI and T. KOKUBO, *J. Amer. Ceram. Soc.* **78** (1995) 2405.
11. T. KOKUBO, *J. Non-Cryst. Solids* **11** (1990) 138.
12. H. KUSHITANI, C. OHTSUKI, S. SAKKA and T. YAMAMURA, *J. Mater. Sci. Mater. Med.* **3** (1992) 79.
13. W. NEUMAN and M. NEUMAN, in ‘‘The Chemical Dynamics of Bone Mineral’’, (University of Chicago, Chicago, IL, 1958) p. 175.
14. K. HATA, T. KOKUBO, T. NAKAMURA and Y. YAMAMURA, *J. Amer. Ceram. Soc.* **78** (1995) 1049.
15. A. PAUL and M. S. ZAMAN, *J. Mater. Sci.* **13** (1978) 1499.
16. Y. EBISAWA, T. KOKUBO, K. OHURA and Y. YAMAMURA, *J. Mater. Sci. Mater. Med.* **1** (1990) 239.
17. T. KOMATSU and N. SOGA, *J. Mater. Sci.* **19** (1984) 2353.
18. *Idem.*, *J. Chem. Phys.* **72** (1980) 1781.
19. Y. EBISAWA, Y. SUGIMOTO, T. HAYASHI, T. KOKUBA, K. OHURA and T. YAMAMURA, *J. Ceram. Soc. Jpn* **99** (1991) 7.

Received 21 November 1997
and accepted 31 August 1998